

Received January 15, 2020, accepted March 19, 2020, date of publication March 31, 2020, date of current version April 15, 2020.

Digital Object Identifier 10.1109/ACCESS.2020.2984528

# Frequency-Weighted Residual Truncation and Padé Approximant for Model Reduction of Power System with Constant Time Delay

YONGHUI NIE<sup>1</sup>, (Member, IEEE), ZHUNHANG WANG<sup>2</sup>, LEI GAO<sup>3</sup>,  
JIANG LI<sup>2</sup>, AND YAN ZHAO<sup>2</sup>

<sup>1</sup>Academic Administration Office, Northeast Electric Power University, Jilin 132012, China

<sup>2</sup>College of Electrical Engineering, Northeast Electric Power University, Jilin 132012, China

<sup>3</sup>China Electric Power Research Institute, Beijing 100192, China

Corresponding authors: Yonghui Nie (nieyonghui@neepu.edu.cn) and Jiang Li (lijiang@neepu.edu.cn)

This work was supported in part by the National Natural Science Foundation of China under Grant 51577023, Grant 61973072, and Grant 51977030, and in part by the “13th Five-Year” Scientific and Technology Research Project of Jilin Province Department of Education under Grant JJKH20180445KJ.

**ABSTRACT** To improve the efficiency for managing power systems with constant time delay, an improved frequency-weighted model reduction is proposed. First, the Padé approximant allows to represent the time delay in the state-space form and build a linear model of the closed-loop power system containing a wide-area damping controller. Then, a weight function is introduced to solve the equilibrium transformation matrix and balance the original system. Finally, the residual order reduction is applied to the model of the power system considering time delay. The proposed method is evaluated in the two-area four-machine test system and New England system, and the effectiveness of the proposed reduction method is verified.

**INDEX TERMS** Frequency weighting, model reduction, Padé approximant, time delay.

## I. INTRODUCTION

The increasing scale of modern power systems and adoption of power system stabilizers, flexible ac transmission systems, high-voltage dc transmission, and a myriad of control methods make the dimension of the state variables to sharply increase [1]–[3]. The development of phasor measurement units and wide-area measurement systems have enabled remote feedback signals with improved observability to provide the conditions for large-scale power systems suppressing inter-area low-frequency oscillations [4], [5]. However, remote signals impose transmission delays ranging from tens to hundreds of milliseconds, which may seriously degrade the power system performance [6]–[9]. Therefore, preventing abrupt dimension increase in a large-scale power system subject to time delay is essential for guaranteeing stability and proper control.

Model reduction is a mathematical approach that can be applied to power systems for solving the curse of

dimensionality and aims to retrieve a reduced-order model that resembles the original model by maintaining inherent characteristics such as passivity and stability. Several model reduction methods for linear time-invariant systems have been applied to power systems, including singular value perturbation [10], moment matching [11], [12], Krylov subspace [13], linear inequality, Hankel optimal method [14], [15], and balanced truncation [16], [17]. Among these methods, balanced truncation is widely used because it maintains system stability and directly provides an expression of the error between the original and reduced system. This method first establishes Lyapunov equations corresponding to the stable linear time-invariant system, whose solution provides a controllable and observable Gramian matrix, and its Cholesky decomposition allows to obtain the equilibrium transformation matrix. Finally, the original system is converted into a balanced system, and the Hankel singular values are used to remove state variables with relatively small influence on the system. Ideally, balanced truncation bounds the error over the entire frequency range. However, as the controlled system works within a specific range, only the

The associate editor coordinating the review of this manuscript and approving it for publication was Junjian Qi.

error in the operating frequency should be considered to further improve model reduction. In fact, further research on balanced order reduction has resulted in frequency-weighted balanced truncation [18], [19].

Enns [19] was the first to extend balanced truncation to include frequency weighting. By introducing input or output weighting matrices, or both, this method can realize model reduction within a specific frequency range. With either input or output weighting, stability of the reduced order model is guaranteed. However, combined input and output weighting may yield unstable models from stable original systems. To prevent potential instability, Lin and Chiu [20] proposed a new technique that yields stable models under input and output weighting, but this approach is limited to strictly proper weights. Their technique was later generalized by Sreeram *et al.* [21] to overcome this limitation. However, these two techniques achieve the computation of error bounds iteratively, and their formulation is highly complicated. Another scheme [22] has been proposed to not only guarantee stability under bilateral weighting but also easily compute error bounds. These methods, however, eliminate states associated with small Hankel singular values, resulting in increased steady-state error.

In this study, we addressed model reduction of power system considering constant time delay in the range of low-frequency oscillations. This method has the following advantages: (I) establishes a linear model of the power system using the Padé approximant, (II) guarantees stability of the reduced-order model under input and output weighting, (III) effectively approximates the behavior of the original system regarding low-frequency oscillations, and (IV) employs the reduced-order method with frequency-weighted residuals in model reduction of the power system with time delay to reduce the steady-state error. The effectiveness of the proposed method is verified in the two-area four-machine system and New England system.

## II. CONTROL OF POWER SYSTEM WITH TIME DELAY

Consider the wide-area closed-loop control system shown in Figure 1. Its open-loop state-space representation is given by

$$\begin{cases} pX_1(t) = A_1X_1(t) + B_1U_1(t) \\ Y_1(t) = C_1X_1(t) \end{cases} \quad (1)$$

where  $p$  represents the derivative of state variables,  $U_1 \in \mathbf{R}^{p \times 1}$ ,  $Y_1 \in \mathbf{R}^{q \times 1}$ , and  $X_1 \in \mathbf{R}^{n_1 \times 1}$  are the input, output, and state vectors of the open-loop power system, respectively, and  $A_1 \in \mathbf{R}^{n_1 \times n_1}$ ,  $B_1 \in \mathbf{R}^{n_1 \times p}$ , and  $C_1 \in \mathbf{R}^{q \times n_1}$  are its state, input, and output matrices, respectively.

The state-space representation of the wide-area closed-loop controller is given by

$$\begin{cases} pX_2(t) = A_2X_2(t) + B_2U_2(t) \\ Y_2(t) = C_2X_2(t) \end{cases} \quad (2)$$

where  $U_2 \in \mathbf{R}^{m \times 1}$ ,  $Y_2 \in \mathbf{R}^{p \times 1}$ , and  $X_2 \in \mathbf{R}^{n_2 \times 1}$  are the input, output, and state vectors of the controller, respectively, with

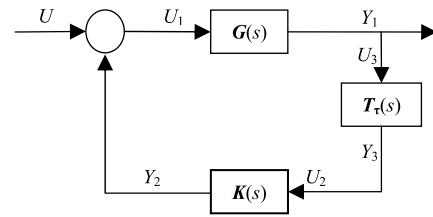


FIGURE 1. Block diagram of closed-loop power system with time delay.

$A_1 \in \mathbf{R}^{n_2 \times n_2}$ ,  $B_2 \in \mathbf{R}^{n_2 \times m}$ , and  $C_2 \in \mathbf{R}^{p \times n_2}$  being its state, input, and output matrices, respectively.

When the power system is controlled using wide-area measurement signals, the closed-loop control becomes a time-delay system given the signal transmission delay. When a control system has time delay, control is sharply degraded can even cause instability, and thus time delay can adversely impact the control system. The delay term can be expressed as  $e^{-s\tau}$  in the Laplace domain, and using the Padé approximant we obtain

$$\begin{aligned} e^{-s\tau} &\approx R(s) \\ &= \sum_{j=0}^l \frac{(l+k-j)!l!(-s\tau)^j}{j!(l-j)!} / \sum_{j=0}^k \frac{(l+k-j)!k!(s\tau)^j}{j!(k-j)!} \end{aligned} \quad (3)$$

where  $R(s)$  is the Padé approximation, and  $l$  and  $k$  represent the order of approximation (usually  $l = k$ ), with larger order making  $R(s)$  approach to  $e^{-s\tau}$ . The Padé approximant is equivalent to filtering pure delay, and smaller delays improve consistency of the phase interval, i.e., a wider filter band implies a higher degree of delay approximation.

The state-space representation of the delay based on the Padé approximant is given by

$$\begin{cases} pX_3(t) = A_3X_3(t) + B_3U_3(t) \\ Y_3(t) = C_3X_3(t) + D_3U_3(t) \end{cases} \quad (4)$$

where  $U_3 \in \mathbf{R}^{q \times 1}$ ,  $Y_3 \in \mathbf{R}^{m \times 1}$ , and  $X_3 \in \mathbf{R}^{n_3 \times 1}$  are the input, output, and state vectors of  $R(s)$ , respectively, and  $A_3 \in \mathbf{R}^{n_3 \times n_3}$ ,  $B_3 \in \mathbf{R}^{n_3 \times q}$ , and  $C_3 \in \mathbf{R}^{m \times n_3}$  are its state, input, and output matrices, respectively.

Hence, using the Padé approximant, the time-delay term is represented in state space, and the wide-area damping controller is used for feedback control of the power system, thus forming a linear model for the closed-loop power system with time delay:

$$\begin{cases} pX(t) = AX(t) + BU_R(t) \\ Y(t) = CX(t) \end{cases} \quad (5)$$

where  $A = \begin{bmatrix} A_1 & -B_1C_2 & 0 \\ B_2D_3C_1 & A_2 & B_2C_3 \\ B_3C_1 & 0 & A_3 \end{bmatrix}$ ,  $B = [B_1 \ 0 \ 0]^T$ ,  $C = [C_1 \ 0 \ 0]$ , and  $X(t) = [X_1(t) \ X_2(t) \ X_3(t)]^T$ .

### III. FREQUENCY-WEIGHTED BALANCED REDUCTION METHOD

The minimal realization of stable linear time-invariant system  $G(s)$  is  $(A, B, C, D)$ . Similarly, the transfer functions of stable input weighting function  $W_i(s)$  and output weighting function  $W_o(s)$  are given by minimal realizations  $(A_i, B_i, C_i, D_i)$  and  $(A_o, B_o, C_o, D_o)$ , respectively. If no pole-zero cancellation occurs, the minimal realization of augmented systems  $G(s)W_i(s)$  and  $W_o(s)G(s)$  can be expressed as

$$G(s)W_i(s) = \begin{bmatrix} \bar{A}_i & \bar{B}_i \\ \bar{C}_i & \bar{D}_i \end{bmatrix} = \begin{bmatrix} A & BC_i & BD_i \\ 0 & A_i & B_i \\ C & DC_i & DD_i \end{bmatrix} \quad (6)$$

$$W_o(s)G(s) = \begin{bmatrix} \bar{A}_o & \bar{B}_o \\ \bar{C}_o & \bar{D}_o \end{bmatrix} = \begin{bmatrix} A & 0 & B \\ B_oC & A_o & B_oD \\ D_oC & C_o & D_oD \end{bmatrix} \quad (7)$$

Let  $\bar{P}_i$  and  $\bar{Q}_o$  satisfy the following Lyapunov equations:

$$\bar{A}_i\bar{P}_i + \bar{P}_i\bar{A}_i^T + \bar{B}_i\bar{B}_i^T = 0 \quad (8)$$

$$A_o^T\bar{Q}_o + \bar{Q}_oA_o + \bar{C}_o^T\bar{C}_o = 0 \quad (9)$$

where  $\bar{P}_i = \begin{bmatrix} P_{11} & P_{12} \\ P_{12}^T & P_{22} \end{bmatrix}$  and  $\bar{Q}_o = \begin{bmatrix} Q_{11} & Q_{12} \\ Q_{12}^T & Q_{22} \end{bmatrix}$  are their block matrix representation. Lyapunov (8) and (9) can be expanded, and their first blocks satisfy:

$$AP_{11} + P_{11}A^T + X = 0 \quad (10)$$

$$A^TQ_{11} + Q_{11}A + Y = 0 \quad (11)$$

with

$$X = BC_iP_{12}^T + P_{12}C_i^TB^T + BD_iD_i^TB^T \quad (12)$$

$$Y = Q_{12}B_oC + C^TB_o^TQ_{12}^T + C^TD_o^TD_oC \quad (13)$$

By simultaneously diagonalizing weighted Gramian matrices  $P_{11}$  and  $Q_{11}$  we obtain

$$T^{-1}P_{11}T^{-T} = T^TQ_{11} \\ T = \text{diag}(\sigma_1, \sigma_2, \dots, \sigma_r, \sigma_{r+1}, \dots, \sigma_n) \quad (14)$$

where  $\sigma_1 \geq \sigma_2 \geq \dots \geq \sigma_n \geq 0$  and  $\sigma_r \gg \sigma_{r+1}$ .

The original system is thus transformed into balanced system:

$$\begin{bmatrix} T^{-1}AT & T^{-1}B \\ CT & D \end{bmatrix} = \begin{bmatrix} \bar{A}_{11} & \bar{A}_{12} & \bar{B}_1 \\ \bar{A}_{21} & \bar{A}_{22} & \bar{B}_2 \\ \bar{C}_1 & \bar{C}_2 & D \end{bmatrix} \quad (15)$$

where  $\bar{A}_{11} \in R^{r \times r}$  and the reduced-order model is given by  $G_r(s) = \bar{C}_1(sI - \bar{A}_{11})^{-1}\bar{B}_1 + D$ .

When the matrices in (12) and (13) are not positive semidefinite, this method cannot guarantee the stability of the reduced-order model under bilateral weighting. To solve this problem, the singular value decompositions of symmetric matrices  $X$  and  $Y$  are first obtained as

$$X = USU^T \quad (16)$$

$$Y = VHV^T \quad (17)$$

where  $U$  and  $V$  are orthogonal matrices, and  $S = \text{diag}(s_1, \dots, s_n)$  and  $H = \text{diag}(h_1, \dots, h_n)$  are diagonal matrices. Assuming that  $X$  and  $Y$  have ranks  $i$  and  $j$ , respectively, the following matrices can be defined:

$$\bar{B} = U \text{diag}(|s_1|^{\frac{1}{2}}, \dots, |s_i|^{\frac{1}{2}}, 0, \dots, 0) \quad (18)$$

$$\bar{C} = \text{diag}(|h_1|^{\frac{1}{2}}, \dots, |h_j|^{\frac{1}{2}}, 0, \dots, 0)V^T \quad (19)$$

where  $|s_i| > 0, |h_j| > 0, |s_{i+1}| = 0, |h_{j+1}| = 0$ .

Let frequency-weighted Gramian matrices  $\hat{P}$  and  $\hat{Q}$  satisfy the following Lyapunov equations:

$$A\hat{P} + \hat{P}A^T + \bar{B}\bar{B}^T = 0 \quad (20)$$

$$\hat{Q}A + A^T\hat{Q} + \bar{C}^T\bar{C} = 0 \quad (21)$$

It can be proved that  $\hat{P}$  and  $\hat{Q}$  are positive definite, and  $(A, \bar{B}, \bar{C})$  is the minimal realization if  $A$  is stable. Therefore,  $\hat{P}$  and  $\hat{Q}$  can be simultaneously diagonalized to obtain balanced transformation matrix  $T$ , the equilibrium system in (15), and the frequency-weighted reduced-order system,  $G_r(s)$ . It can also be proved that this method guarantees stability of the reduced-order model under bilateral weighting.

For a balanced system based on Gramian matrix transformation, the Hankel singular values of the system provide a measure of the controllability and observability. When the singular value is relatively large, the control input has a greater impact on the corresponding state and on the output. Therefore, the state corresponding to the maximum singular value has the highest impact on the input and output of the system. Model reduction using balanced truncation eliminates states associated with small Hankel singular values, whose contribution to the system are considered negligible. The reduced-order model with frequency-weighted balanced truncation for the power system is given by

$$p\bar{x}_1 = \bar{A}_{11}\bar{x}_1 + \bar{B}_1u \quad (22)$$

$$y = \bar{C}_1\bar{x}_1 \quad (23)$$

Balanced truncation can ensure a close approximation to the original system in the whole frequency range, but generally it cannot maintain the steady-state performance of the original system. To mitigate the steady-state error, we apply frequency-weighted residual reduction, which consists in considering the derivative of states  $p\bar{x}_2$  associated with small singular values in (16) as null while keeping the remainder of the system unchanged. As a result, the following reduced-order model of the system is obtained:

$$\begin{bmatrix} p\bar{x}_1 \\ 0 \end{bmatrix} = \begin{bmatrix} \bar{A}_{11} & \bar{A}_{12} \\ \bar{A}_{21} & \bar{A}_{22} \end{bmatrix} \begin{bmatrix} \bar{x}_1 \\ \bar{x}_2 \end{bmatrix} + \begin{bmatrix} \bar{B}_1 \\ \bar{B}_2 \end{bmatrix} u \quad (24)$$

$$y = [\bar{C}_1 \quad \bar{C}_2] \begin{bmatrix} \bar{x}_1 \\ \bar{x}_2 \end{bmatrix} + Du \quad (25)$$

which are differential algebraic equations and can be expressed as the following residual reduced-order models:

$$p\bar{x}_1 = \hat{A}\bar{x}_1 + \hat{B}u \quad (26)$$

$$y = \hat{C}\bar{x}_1 + \hat{D}u \quad (27)$$

where  $\hat{A} = \bar{A}_{11} - \bar{A}_{12}\bar{A}_{22}^{-1}\bar{A}_{21}$ ,  $\hat{B} = \bar{B}_1 - \bar{A}_{12}\bar{A}_{22}^{-1}\bar{B}_2$ ,  $\hat{C} = \bar{C}_1 - \bar{C}_2\bar{A}_{22}^{-1}\bar{A}_{21}$ , and  $\hat{D} = D - \bar{C}_2\bar{A}_{22}^{-1}\bar{B}_2$ .

For stable linear time-invariant system  $G(s)$  and stable input and output weighting transfer functions  $W_i(s)$  and  $W_o(s)$ , we propose a novel frequency-weighted truncation for model reduction to ensure stability of the resulting model with bilateral weights. For the power system working with in a specific low-frequency oscillation range, 0.1–2.5 Hz, the proposed truncation proceeds as follows:

- 1) Establish the power system model with time delay using the Padé approximant.
- 2) Compute  $P_{11}$  and  $Q_{11}$  according to (8) and (9).
- 3) Compute  $X$  and  $Y$  according to (10) and (11).
- 4) Apply singular value decomposition on matrices  $X$  and  $Y$  to obtain  $USU^T$  and  $VHV^T$ .
- 5) Compute  $\bar{B}$  and  $\bar{C}$  according to (18) and (19).
- 6) Compute  $\hat{P}$  and  $\hat{Q}$  according to (21) and (22).
- 7) Obtain transformation matrix  $T$  simultaneously diagonalizing  $\hat{P}$  and  $\hat{Q}$  like in (14).
- 8) Transform and partite the original system like in (15).
- 9) Determine the resulting reduced model,  $G_r(s) = \hat{C}(sI - \hat{A})^{-1}\hat{B} + \hat{D}$ , which is stable.

The error bound between the reduced and original system can be expressed as

$$\|W_o(s)(G(s) - G_r(s))W_i(s)\|_\infty \leq 2 \|W_o(s)L\|_\infty \|KW_i(s)\|_\infty \sum_{i=r+1}^n \sigma_i \quad (28)$$

where  $K = \text{diag}(|s_1|^{-1/2}, \dots, |s_j|^{-1/2}, 0, \dots, 0)U^T B$  and  $L = CV \text{diag}(|h_1|^{-1/2}, \dots, |h_j|^{-1/2}, 0, \dots, 0)$ .

Both the frequency-weighted and residual truncation have the same error bounds but exhibit different high- and low-frequency characteristics. Specifically, the former has better model matching in high frequencies, whereas the latter has better matching in low frequencies.

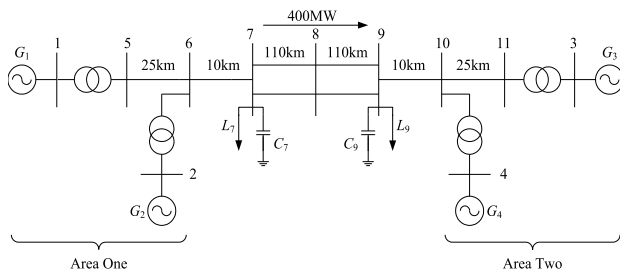


FIGURE 2. Diagram of the two-zone four-machine power system.

## IV. SIMULATION RESULTS

### A. TWO-AREA FOUR-MACHINE SYSTEM

We used the two-zone four-machine system, shown in Figure 2, to verify the effectiveness of the proposed method with the detailed parameters given by Kundur [1]. The generators adopt a fourth-order model and are equipped with

TABLE 1. Electromechanical mode analysis of the two-area four-machine power system

Mode	Type	Damping ratio	Frequency (Hz)
1	Local	0.0425	1.0146
2	Local	0.0446	1.0454
3	Inter-area	-0.0177	0.5945

a fourth-order static excitation system, and the power system stabilizer also adopts a fourth-order model. The test system is linearized under normal operation, and the critical eigenvalues are numerically obtained for the open-loop system. Table 1 lists the three electromechanical modes of the system, where modes 1 and 2 are local-oscillation modes with poor damping, and mode 3 is an inter-area oscillation mode, whose damping is negative. By using the residue matrix method, units 1 and 2 of the system contain local power system stabilizers to improve the damping ratio of local modes, and the velocity deviation of unit 1 and excitation system of unit 3 support wide-area control by damping the inter-area mode. Assuming a remote signal transmission delay of 0.03 s, the model of the power system considering the time delay is established using the twentieth-order Padé approximant. We obtained  $\sigma_7 \gg \sigma_8$  from the Hankel singular values, and hence the order for the frequency-weighted truncation is seven. We evaluated frequency-weighted truncation and residual truncation as order-reduction methods for the time-delay model, as detailed in the sequel.

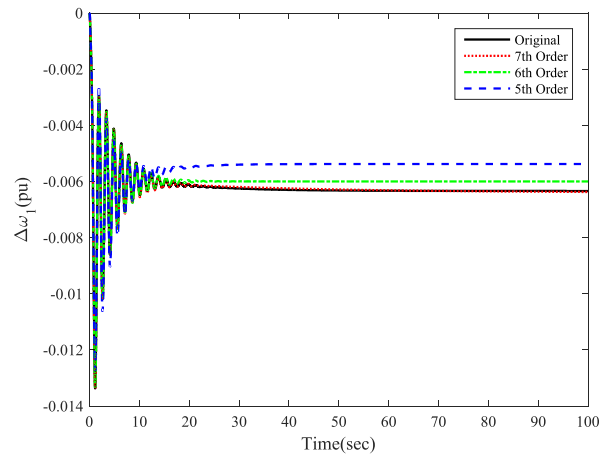


FIGURE 3. Step response for frequency-weighted truncation.

Frequency-weighted truncation can be used for model reduction of the time-delay power system. Figures 3 to 5 show the step response of the angular velocity deviation for unit 1 along with the amplitude (in decibels) and phase (in degrees) characteristics according to the frequency in logarithmic scale from the original and reduced-order systems.

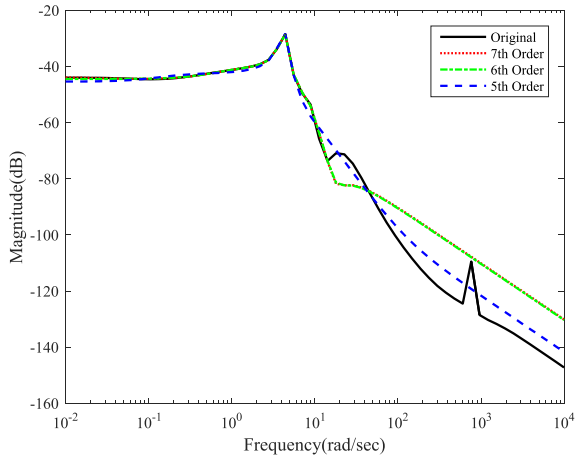


FIGURE 4. Amplitude–frequency characteristic for frequency-weighted truncation.

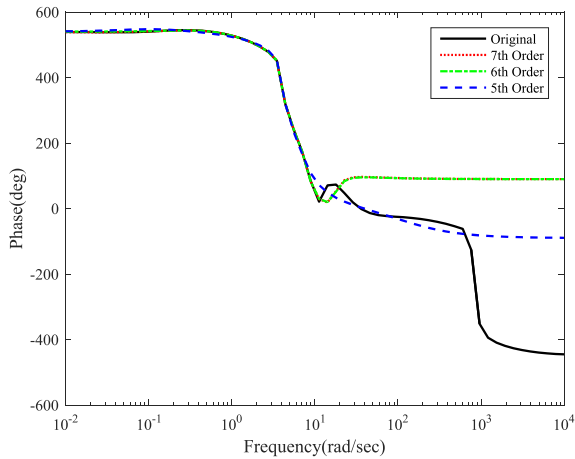


FIGURE 5. Phase–frequency characteristic for frequency-weighted truncation.

The response of the seventh-order reduced system is basically the same as that of the original system, because it preserves the high-frequency components at the initial stage of the response and provides a consistent phase in steady state. For the fifth- and sixth-order reduced systems, the step response exhibits some stability error, and the transient phase of the step response is slightly different from that of the original system. From the frequency response, we can further verify error in the low-frequency band, whereas the high-frequency band error is relatively large, and the high-frequency amplitudes of the two reduced systems have a similar considerable decline compared to the original system, resulting in the abovementioned time-domain changes of the two reduced systems. We do not show the response curve from the eighth-order system onwards, as it is basically the same as that of the original system. Likewise, for frequencies below 10 Hz, the response of the reduced-order systems is very close to that of the original system, thus reflecting the low-frequency oscillations. In contrast, for frequencies above 10 Hz, the error between the frequency-weighted reduced system and the

original system gradually increases. Nevertheless, model reduction preserves the important low-frequency oscillation characteristics of the power system.

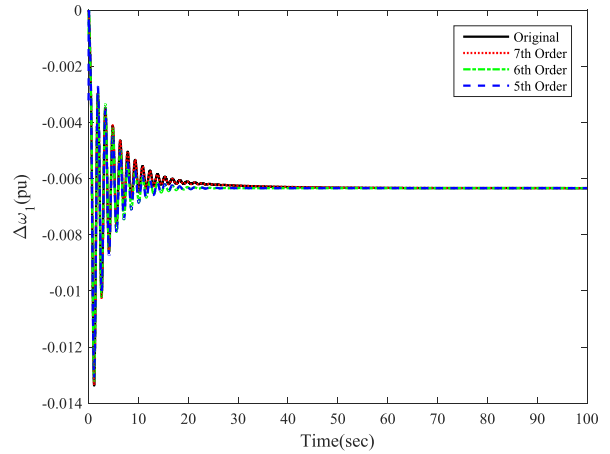


FIGURE 6. Step response for frequency-weighted residual truncation.

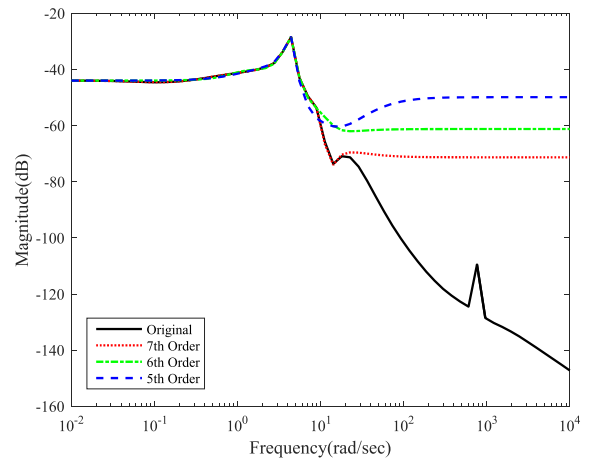


FIGURE 7. Amplitude–frequency characteristic for frequency-weighted residual truncation.

We also evaluated the frequency-weighted residual truncation to verify its performance improvement. Figures 6 to 8 show the step response of the angular velocity deviation for unit 1 and the frequency characteristics from the original and each reduced system. Compared with the conventional truncation, the frequency-weighted residual truncation reduces the steady-state error of each reduced system, providing more consistency in the step response to the original system in steady state and improves accuracy of the steady-state approximation. Figures 7 and 8 show that the frequency-weighted residual truncation improves the model reduction performance in low frequencies, with the components agreeing with those of the original system, further verifying the effectiveness of the reduction to reflect low-frequency oscillations of the power system. However, residual truncation leads to relatively large errors in high frequencies and deviation in the transition phase of the step response.

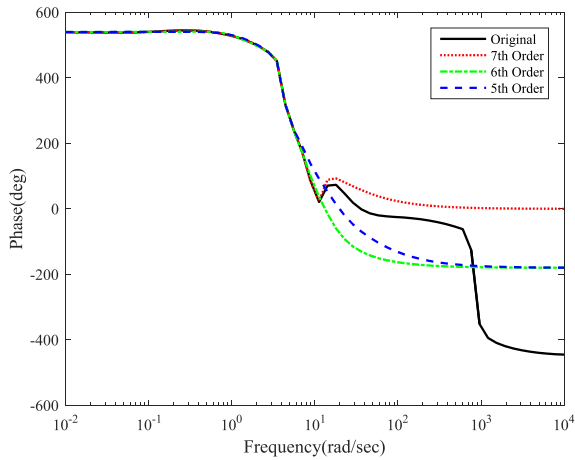


FIGURE 8. Phase-frequency characteristic for frequency-weighted residual truncation.

Overall, given the close relation of low-frequency oscillation to weakly damping electromechanical oscillation modes, the installation site and input signal of the controller selected using residue matrix method result in high observability and controllability of these modes, whose state variables retrieve large Hankel singular values with effects reflected in the reduced-order model. On the other hand, the differential equations of state variables associated with small Hankel singular values are converted into steady-state equations. Hence, the proposed method not only retains the frequency characteristics of low-frequency oscillations in power systems, but also greatly improves the accuracy of the step response in a steady state of the reduced system.

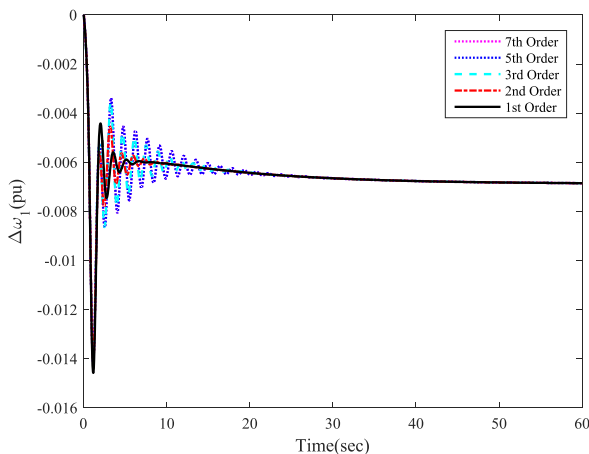


FIGURE 9. Effect of Padé approximant order on frequency-weighted residual truncation.

Considering a delay of 0.1 s and Padé approximants of orders 1, 2, 3, 5, and 7 to establish the linear model of the power system considering the time delay, we evaluated the approximant effect on frequency-weighted residual truncation for model reduction. The order of the reduced system is determined when a pair of singular values satisfy  $\sigma_r \gg \sigma_{r+1}$ . The simulation results of this evaluation are shown in Figure 9. As the approximant order of time delay

increases, the oscillation of the step response becomes more prominent and longer during the transition process. For orders above three, the dynamics of the reduced systems tend to be consistent, showing that third- or higher-order Padé approximants can meet the frequency band requirements of the power system. Note that the step responses of the reduced systems exhibit almost the same steady-state process by the use of frequency-weighted residual truncation.

**B. NEW ENGLAND SYSTEM**

We selected the New England system consisting of 10 units, shown in Figure 10, to further evaluate the effectiveness of the proposed reduction method. One of the units is equivalent to machine  $G_{10}$  of the US–Canada interconnection system. In this paper,  $G_{10}$  adopts a second-order model, and the other units adopt the same model as the two-area four-machine system. More details on the New England system can be found in Ref. 23.

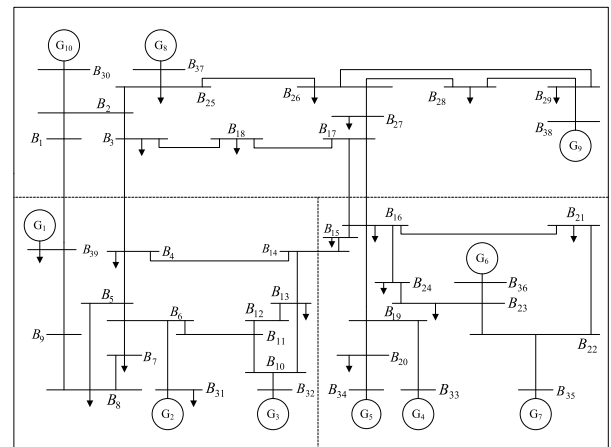


FIGURE 10. Diagram of the New England system.

The test system has linear behavior under normal operation, and the critical eigenvalues can be numerically obtained. Table 2 lists the nine electromechanical modes of the system, where modes 1–6 are local oscillation modes, and modes 7–9 are inter-area oscillation modes. As the system has a positive damping by the excitation systems of the generators, it remains stable under open loop operation. However, given its lower oscillation frequency compared to the other modes, inter-area mode 9 belongs to the dominant mode with slowest decay, with generator  $G_{10}$  swinging against the generator group comprising  $G_1$  to  $G_9$ . Therefore, the excitation system of  $G_9$  and relative angular velocity  $\Delta\omega_{10-7}$  were selected to constitute feedback control to damp inter-area oscillations.

For a remote signal transmission delay of 0.03 s, the model of the power system considering the time delay was obtained using the twentieth-order Padé approximant. We obtained from the Hankel singular values, and hence the order for the frequency-weighted truncation is 16. We first evaluated frequency-weighted truncation as order-reduction method for the time-delay model. Figures 11 to 13 show

**TABLE 2.** Electromechanical mode analysis of the New England system.

Mode	Type	Damping ratio	Frequency (Hz)
1	Local	0.0759	1.5263
2	Local	0.0555	1.4893
3	Local	0.0645	1.4271
4	Local	0.0565	1.2715
5	Local	0.0479	1.2454
6	Local	0.0392	1.1935
7	Inter-area	0.0281	1.1099
8	Inter-area	0.0227	1.0499
9	Inter-area	0.0245	0.6793

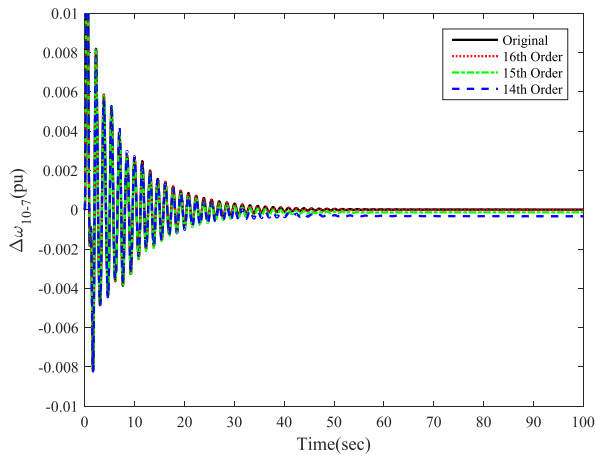


**FIGURE 11.** Step response for frequency-weighted truncation.

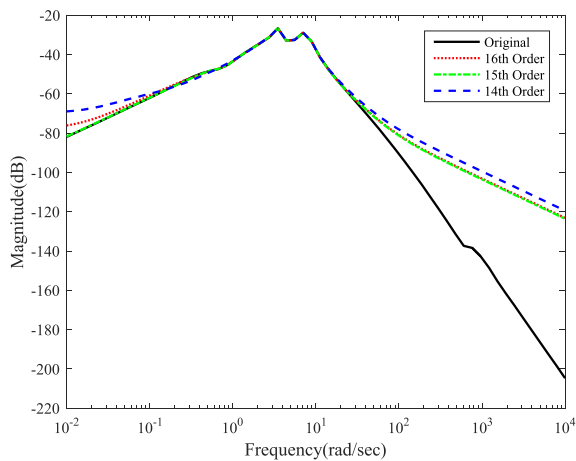


**FIGURE 12.** Amplitude-frequency characteristic for frequency-weighted truncation.

the step response of the angular velocity deviation  $\Delta\omega_{10-7}$  and the frequency characteristics from the original and reduced-order systems. Similar results to the two-area four-machine system are obtained, that is, the response of the 16th-order reduced system is basically the same as that of the original system in the transient and steady-state regimes. For reduced systems with lower order, the step response exhibits some stability error, but the transient regime from the step response is slightly different from that of the original system, as demonstrated by the frequency characteristics.

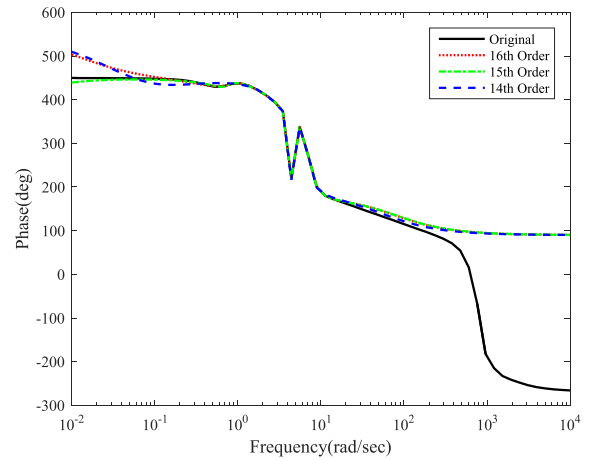


**FIGURE 13.** Phase-frequency characteristic for frequency-weighted truncation.

Similarly, frequency response shows that model reduction preserves important low-frequency oscillation characteristics of the power system.

To further evaluate the performance improvement from frequency-weighted residual truncation, Figures 14 to 16 show the step response of the angular velocity deviation  $\Delta\omega_{10-7}$  and the frequency characteristics from the original and each reduced system. As mentioned above, frequency-weighted residual truncation reduces the steady-state error of the system compared to conventional truncation, providing a more consistent step response with that of the original system in steady state and improving the model reduction performance in low frequencies, thereby preserving low-frequency oscillations of the power system. However, residual truncation leads to relatively large errors in high frequencies and deviation in the transition phase of the step response.

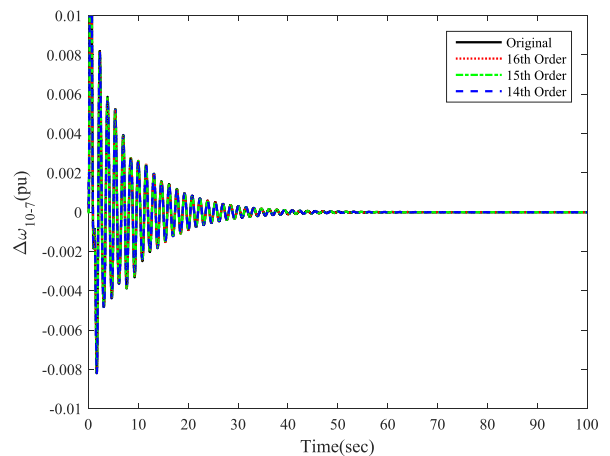


**FIGURE 14.** Step response for frequency-weighted residual truncation.

We used a delay of 0.1 s to establish the linear model of the power system considering the time delay and investigate the effect of the approximant order on frequency-weighted

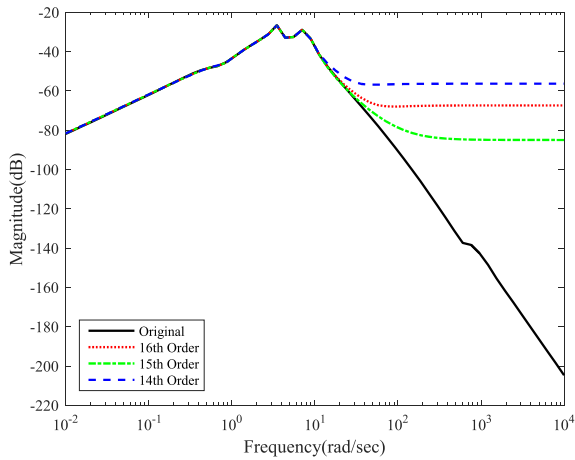


FIGURE 15. Amplitude–frequency characteristics for frequency-weighted residual truncation.

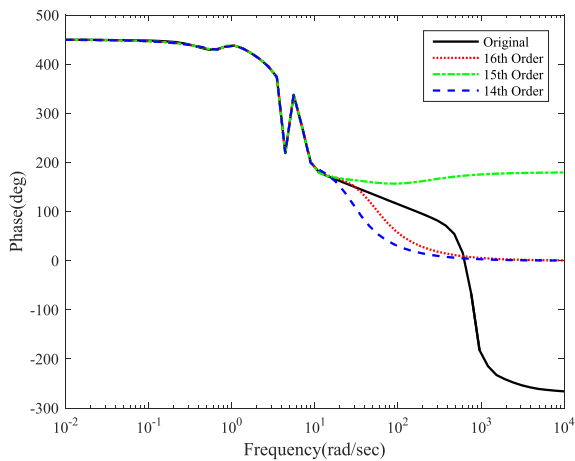


FIGURE 16. Phase–frequency characteristics for frequency-weighted residual truncation.

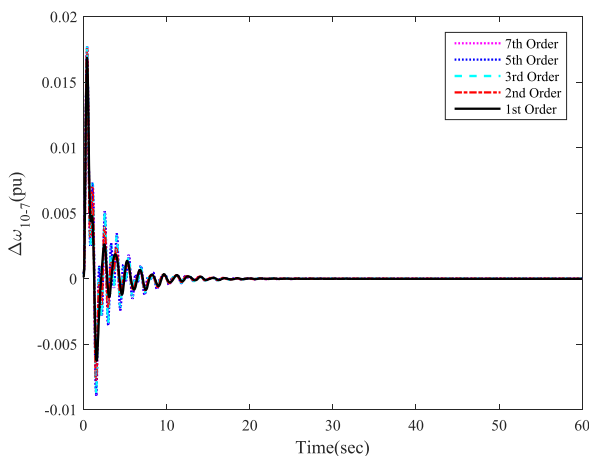


FIGURE 17. Effect of Padé approximant order on frequency-weighted residual truncation.

residual truncation for model reduction, whose results are shown in Figure 17. Similar results to the previous evaluation were obtained, that is, frequency-weighted residual

truncation exhibits almost the same steady-state response in the reduced systems, and third- or higher-order Padé approximants can meet the frequency band requirements of the power system.

### V. CONCLUSION

A power system linearization model considering constant time delay based on the Padé approximant is proposed. In addition, model reduction is performed using frequency-weighted residual truncation. Simulation results show that the proposed method has the following features. The method guarantees that the reduced-order models under input and output weighting are stable. Residual truncation greatly reduces error in steady state, making the steady-state step response of the reduced system to closely approach that of the original system. The frequency characteristic of the reduced system is closer to that of the original system in the range of low-frequency oscillations. A Padé approximant of at least the third order can satisfy power system requirements for the frequency-weighted residual order reduction.

Current research is limited to model reduction methods for linear time-invariant systems. From the results in this study, we will focus on model reduction of interval systems to then apply model reduction.

### ACKNOWLEDGMENT

The authors would like to thank Editage (www.editage.cn) for English language editing.

### REFERENCES

- [1] P. Kundur, *Power System Stability and Control*. New York, NY, USA: McGraw-Hill, 1994.
- [2] A. I. Konara and U. D. Annakkage, “Robust power system stabilizer design using eigenstructure assignment,” *IEEE Trans. Power Syst.*, vol. 31, no. 3, pp. 1845–1853, May 2016.
- [3] P. Kundur, M. Klein, G. J. Rogers, and M. S. Zywno, “Application of power system stabilizers for enhancement of overall system stability,” *IEEE Power Eng. Rev.*, vol. 9, no. 5, p. 61, May 1989.
- [4] S. Song, J. Liu, and H. Wang, “Adaptive neural network control for uncertain switched nonlinear systems with time delays,” *IEEE Access*, vol. 6, pp. 22899–22907, 2018.
- [5] X. Zhang, B. Li, G. Zhu, X. Chen, and M. Zhou, “Decentralized adaptive quantized excitation control for multi-machine power systems by considering the line-transmission delays,” *IEEE Access*, vol. 6, pp. 61918–61933, 2018.
- [6] W. Yao, L. Jiang, J. Wen, Q. H. Wu, and S. Cheng, “Wide-area damping controller of FACTS devices for inter-area oscillations considering communication time delays,” *IEEE Trans. Power Syst.*, vol. 29, no. 1, pp. 318–329, Jan. 2014.
- [7] S. Wang, X. Meng, and T. Chen, “Wide-area control of power systems through delayed network communication,” *IEEE Trans. Control Syst. Technol.*, vol. 20, no. 2, pp. 495–503, Mar. 2012.
- [8] J. Cai, J. Wan, H. Que, Q. Zhou, and L. Shen, “Adaptive actuator failure compensation control of second-order nonlinear systems with unknown time delay,” *IEEE Access*, vol. 6, pp. 15170–15177, 2018.
- [9] H. Ye, Y. Liu, and P. Zhang, “Efficient eigen-analysis for large delayed cyber-physical power system using explicit infinitesimal generator discretization,” *IEEE Trans. Power Syst.*, vol. 31, no. 3, pp. 2361–2370, May 2016.
- [10] S. Wang, S. Lu, N. Zhou, G. Lin, M. Elizondo, and M. A. Pai, “Dynamic-feature extraction, attribution, and reconstruction (DEAR) method for power system model reduction,” *IEEE Trans. Power Syst.*, vol. 29, no. 5, pp. 2049–2059, Sep. 2014.

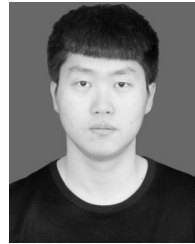


- [11] T. C. Ionescu and A. Astolfi, "Moment matching for nonlinear port Hamiltonian and gradient systems," *IFAC Proc. Volumes*, vol. 46, no. 23, pp. 395–399, 2013.
- [12] T. C. Ionescu, A. Astolfi, and P. Colaneri, "Families of moment matching based, low order approximations for linear systems," *Syst. Control Lett.*, vol. 64, pp. 47–56, Feb. 2014.
- [13] D. Chaniotis and M. A. Pai, "Model reduction in power systems using Krylov subspace methods," *IEEE Trans. Power Syst.*, vol. 20, no. 2, pp. 888–894, May 2005.
- [14] S. Lall, J. E. Marsden, and S. Glavaški, "A subspace approach to balanced truncation for model reduction of nonlinear control systems," *Int. J. Robust Nonlinear Control*, vol. 12, no. 6, pp. 519–535, May 2002.
- [15] J. H. Chow, *Power System Coherency and Model Reduction*. New York, NY, USA: Springer, 2013.
- [16] J. Qi, J. Wang, H. Liu, and A. D. Dimitrovski, "Nonlinear model reduction in power systems by balancing of empirical controllability and observability covariances," *IEEE Trans. Power Syst.*, vol. 32, no. 1, pp. 114–126, Jan. 2017.
- [17] C. Sturk, L. Vanfretti, Y. Chompoobutgool, and H. Sandberg, "Coherency-independent structured model reduction of power systems," *IEEE Trans. Power Syst.*, vol. 29, no. 5, pp. 2418–2426, Jun. 2014.
- [18] P. Benner, D. C. Sorensen, and V. Mehrmann, *Dimension Reduction of Large-Scale Systems* (Lecture Notes in Computational Science and Engineering). Berlin, Germany: Springer, 2005.
- [19] D. Enns, "Model reduction with balanced realizations: An error bound and a frequency weighted generalization," in *Proc. 23rd IEEE Conf. Decis. Control*, Las Vegas, Nevada, USA, Dec. 1984, pp. 127–132.
- [20] C. A. Lin and T. Y. Chiu, "Model-reduction via frequency weighted balanced realization," *Control-Theory Adv. Technol.*, vol. 8, no. 2, pp. 341–351, Jun. 1992.
- [21] V. Sreeram, B. D. O. Anderson, and A. G. Madievski, "New results on frequency weighted balanced reduction technique," in *Proc. Amer. Control Conf. (ACC)*, Seattle, WA, USA, 1995, pp. 4004–4009.
- [22] A. Varga and B. D. O. Anderson, "Accuracy-enhancing methods for balancing-related frequency-weighted model and controller reduction," *Automatica*, vol. 39, no. 5, pp. 919–927, May 2003.
- [23] P. Bueno de Araujo and L. C. Zanetta, "Pole placement method using the system matrix transfer function and sparsity," *Int. J. Electr. Power Energy Syst.*, vol. 23, no. 3, pp. 173–178, Mar. 2001.



**YONGHUI NIE** (Member, IEEE) received the M.Eng. degree in electrical engineering from Northeast Electric Power University, Jilin, China, in 2006, and the Ph.D. degree in electrical engineering from Xi'an Jiaotong University, Xi'an, China, in 2014.

He has been a Professor with Northeast Electric Power University, since 2018. His current research interests include optimal operation, stability analysis, and control of power systems.



**ZHUNHANG WANG** received the B.S. degree in electrical engineering from Northeast Electric Power University, Jilin, China, in 2018.

He is currently a Research Student in electrical engineering with Northeast Electric Power University. His research interests include optimal operation, stability analysis, and control of power systems.



**LEI GAO** was born in Shandong, China, in 1980. He received the M.S. degree from Northeast Electric Power University, China, in 2006, and the Ph.D. degree from Shandong University, China, in 2014.

He is currently a Professor of the China Electric Power Research Institute (CEPRI). His main research interest includes power system analysis and control.



**JIANG LI** (Member, IEEE) received the B.S. degree from the Shanghai University of Electric Power, Shanghai, China, in 2003, the M.S. degree in electrical engineering from Northeast Electric Power University, Jilin, China, in 2006, and the Ph.D. degree from North China Electric Power University, Beijing, China, in 2010.

He was a Visiting Scholar with Cornell University, Ithaca, NY, USA, for one year. He is currently a Professor with the Department of

Electrical Engineering, Northeast Electric Power University. His research interests include mainly in generation of renewable energy, and operation and control of power systems.



**YAN ZHAO** was born in Jilin City, Jilin, China, in 1974. She received the M.S. degree in power system and its automation from Northeast Electric Power University, Jilin, in 2005, and the Ph.D. degree in power system and its automation from the Harbin Institute of Technology, Harbin, in 2016.

Since 2012, she has been an Assistant Professor with the Power Transmission and Distribution Department, Northeast Electric Power University.

She is the author of a book and more than 20 articles. Her research interests include power system stability analysis and control, application of artificial intelligence in power system and fault signal processing in power systems.

• • •